Using chemical tracers in hillslope soils to estimate the importance of chemical denudation under conditions of downslope sediment transport

Using chemical tracers in hillslope soils to estimate the importance of chemical denudation under conditions of downslope sediment transport

Simon Marius Mudd[1] and David Jon Furbish[2]

Received 1 June 2005; revised 27 February 2006; accepted 9 March 2006; published 20 June 2006.

[1] We present a model of hillslope soils that couples the evolution of topography, soil thickness, and the concentration of constituent soil phases, defined as unique components of the soil with collective mass equal to the total soil mass. The model includes both sediment transport and chemical denudation. A simplified two-phase model is developed; the two phases are a chemically immobile phase, which has far lower solubility than the bulk soil and is not removed through chemical weathering (for example, zircon grains), and a chemically mobile phase that may be removed from the system through chemical weathering. Chemical denudation rates in hillslope soils can be measured using the concentration of immobile elements, but the enrichment of these immobile elements is influenced by spatial variations in chemical denudation rates and spatial variations in the chemical composition of a soil's parent material. These considerations cloud the use of elemental depletion factors and cosmogenic nuclide-based total denudation rates used to identify the relationship between physical erosion and chemical weathering if these techniques do not account for downslope sediment transport. On hillslopes where chemical denudation rates vary in space, estimates of chemical denudation using techniques that do not account for downslope sediment transport and spatial variations in chemical denudation rates may be adequate where the chemical denudation rate is a significant fraction of the total denudation rate but are inadequate in regions where chemical weathering rates are small compared to the total denudation rate. We also examine relationships between transient mechanical and chemical denudation rates. Soil particle residence times may affect chemical weathering rates, and the relationship between total landscape-lowering rates and soil particle residence times can thus be quantified.

Citation: Mudd, S. M., and D. J. Furbish (2006), Using chemical tracers in hillslope soils to estimate the importance of chemical denudation under conditions of downslope sediment transport, *J. Geophys. Res.*, *111*, F02021, doi:10.1029/2005JF000343.

1. Introduction

[2] Many landscapes are mantled by a mobile layer of soil. This soil is created from weathered bedrock or saprolite through a variety of processes such as penetration by tree roots, burrowing by mammals, or freeze-thaw mechanisms [e.g., see *Birkeland*, 1999]. Once created, mobile soil is removed from the landscape by either mechanical sediment transport [e.g., *Gilbert*, 1877] or by chemical weathering processes [e.g., *White and Brantley*, 1995]. Chemical weathering within a hillslope soil plays an important role in the export of dissolved material from basins; recent work has found that the fluxes of solutes from soils may be equal to or greater than the fluxes from saprolite and weathered bedrock [*Anderson et al.*, 2002; *Green et al.*, 2005].

[3] Chemical weathering of silicate minerals can serve as a sink for atmospheric CO_2 [*Berner et al.*, 1983]; studies of chemical weathering therefore have been motivated in part by the hypothesis that there are feedbacks between chemical weathering and global climate [*Raymo and Ruddiman*, 1992]. In their landmark study, *Raymo and Ruddiman* [1992] hypothesized that an increased mechanical denudation rate due to tectonic uplift can result in an increased chemical denudation rate (due to an increase in the rate of production of fresh mineral surfaces) and global cooling (due to reduction in atmospheric CO_2). A number of researchers have demonstrated a coupling between chemical and mechanical denudation rates using stream gauge data [e.g., *Stallard*, 1995; *West et al.*, 2005]. Measurements of both chemical and mechanical denudation rates from stream gauges have the advantage of integrating denudation over an entire basin but have the disadvantage of varying because of the stochastic distribution of floods and brief measurement periods relative to the measurement period

[1]Department of Civil and Environmental Engineering, Vanderbilt University, Nashville, Tennessee, USA.
[2]Department of Earth and Environmental Sciences, Vanderbilt University, Nashville, Tennessee, USA.

0148-0227/06/2005JF000343

needed to fully characterize the full distribution of floods [e.g., *Kirchner et al.*, 2001].

[4] Quantifying the balance between chemical and mechanical denudation in hillslope soils has the advantage of averaging the denudation rate over 10 kyr-1000 kyr, as hillslope soils respond more slowly than channels to erosional forcings by storms [e.g., *Furbish and Fagherazzi*, 2001; *Mudd and Furbish*, 2005]. In the soil environment, mass balance techniques are useful in determining the extent of chemical weathering [e.g., *April et al.*, 1986; *Brimhall and Dietrich*, 1987]. These mass balance techniques involve measuring the enrichment of minerals in the soil that are relatively insoluble. Until recently, quantifying rates of chemical denudation within soils has been limited to nonsloping sites where the age of the soil is known [e.g., *Chadwick et al.*, 1990; *Merritts et al.*, 1992; *Taylor and Blum*, 1995]. A recent series of papers has now shown that the chemical denudation rate may be estimated in eroding landscapes if the total denudation rate (the sum of the chemical and mechanical denudation rates) is known [*Small et al.*, 1999; *Riebe et al.*, 2001, 2003, 2004a, 2004b]. The total denudation rate of a soil may be determined by measuring inventories of cosmogenic radionuclides at the soil-saprolite boundary [e.g., *Heimsath et al.*, 1997; *Small et al.*, 1997]. Measuring the chemical denudation rate using the enrichment of immobile minerals is distinct from solute studies because the estimate of chemical denudation using this method is averaged over the residence time of the soil particles.

[5] While the techniques of *Riebe et al.* [2001] and *Small et al.* [1999] allow for the estimation of the relative proportion of chemical and mechanical weathering in mobile soils averaged over the residence time of the soil particles, they are limited to soils in which there is no spatial variation in the chemical composition of the parent material, and in which the chemical denudation rate in the soil does not vary spatially. Strong spatial covariations of chemical weathering and sediment transport processes, however, have been long inferred from routine observations that soil properties systematically vary along hillslopes [e.g., *Birkeland*, 1999]. Recent investigations have found spatial heterogeneity in the degree and rate of chemical weathering in hillslope soils as a function of position using mass balance techniques [*Green et al.*, 2005; *Nezat et al.*, 2004; *Yoo et al.*, 2004].

[6] In this contribution we extend the work of *Small et al.* [1999] and *Riebe et al.* [2001] by developing a model that explicitly includes spatial variations in chemical denudation rates and spatial variations in the chemical composition of the parent material from which the soil is formed. This new model is used to address several questions. First we examine to what extent the chemical composition of the soil is expected to vary under hypothesized spatial variations in the chemical denudation rate. We then address the question of how closely the chemical denudation rate estimated using the technique of *Riebe et al.* [2001] will match the true basin-averaged chemical denudation rate if the chemical composition of the parent material or the chemical denudation rate varies spatially. Finally, the model is used to examine patterns of soil chemical composition under conditions of transient erosion rates, and how such transient erosion rates may affect the sediment transport and chemical denudation rates of hillslope soils.

2. A Coupled Model of Hillslope Evolution

[7] Our model, which couples the elevation a hillslope surface with the concentration of constituent phases (to be defined in section 2.2) in the soil, is based on conservation of mass for the total soil layer and for each constituent phase within the soil. First we derive a statement of mass conservation for the whole soil.

2.1. Conservation of Total Soil Mass

[8] Many authors have derived equations for conservation of mass on hillslopes that contain terms for the mechanical transport of sediment [*Ahnert*, 1976; *Anderson*, 2002; *Armstrong*, 1976; *Culling*, 1960; *Gabet et al.*, 2003; *Kirkby*, 1971; *Roering et al.*, 2001]. Others have derived models that explicitly include terms for mass loss due to chemical weathering processes [*Kirkby*, 1977, 1985a, 1985b; *Mudd and Furbish*, 2004]. Here we use a depth-integrated equation for the conservation of mass of a hillslope soil, one including both chemical and physical processes:

$$\frac{\partial(h\overline{\rho}_s)}{\partial t} + \frac{\partial(h\overline{v_x\rho_s})}{\partial x} + \frac{\partial\left(h\overline{v_y\rho_s}\right)}{\partial y} - h\overline{S}_v - \rho_\zeta d_\zeta - \rho_r p_\eta = 0, \quad (1)$$

where $h(L)$ is soil depth, $\rho_s(L^3\ T^{-1})$ is the dry bulk density of the soil, $v_x(L\ T^{-1})$ is the velocity of the sediment in the x direction, $v_y(L\ T^{-1})$ is the velocity of the sediment in the y direction, $S_v(M\ T^{-1}\ L^{-3})$ is a rate of mass loss or gain per unit volume due to chemical or biological processes, $\rho_\zeta(M\ L^{-3})$ is the dry bulk density of material deposited at the surface, $d_\zeta(L\ T^{-1})$ is the deposition rate of material at the surface, ρ_r $(M\ L^{-3})$ is the density of the parent material, p_η $(L\ T^{-1})$ is the rate of entrainment of parent material into the active soil layer, and the overbars denote depth-averaged quantities (Figure 1). The derivation of equation (1) is presented in *Mudd and Furbish* [2004]. The first term in equation (1) is the change with respect to time of the mass in a column of soil. The second and third terms are the mass fluxes of sediment in the x and y directions, respectively. The fourth term is the rate of mass lost or gained because of chemical or biological processes (e.g., weathering of minerals, deposition of plant material). The last two terms are rate of mass losses or gains due to deposition of material on the surface of the soil or production of soil at the soil-saprolite boundary. The soil thickness h is defined as the distance between the elevation of the soil surface, ζ (L), and the elevation of the base of the mechanically active layer of the soil, η (L):

$$h = \zeta - \eta, \quad (2)$$

where the mechanically active layer is the portion of the soil which is experiencing mechanical disturbances.

[9] The deposition and production rate terms (d_ζ and p_η, respectively) represent the change in the elevation of the base of the active layer and the surface if the hillslope sediment velocities v_x, v_y, and v_z are zero (the vertical

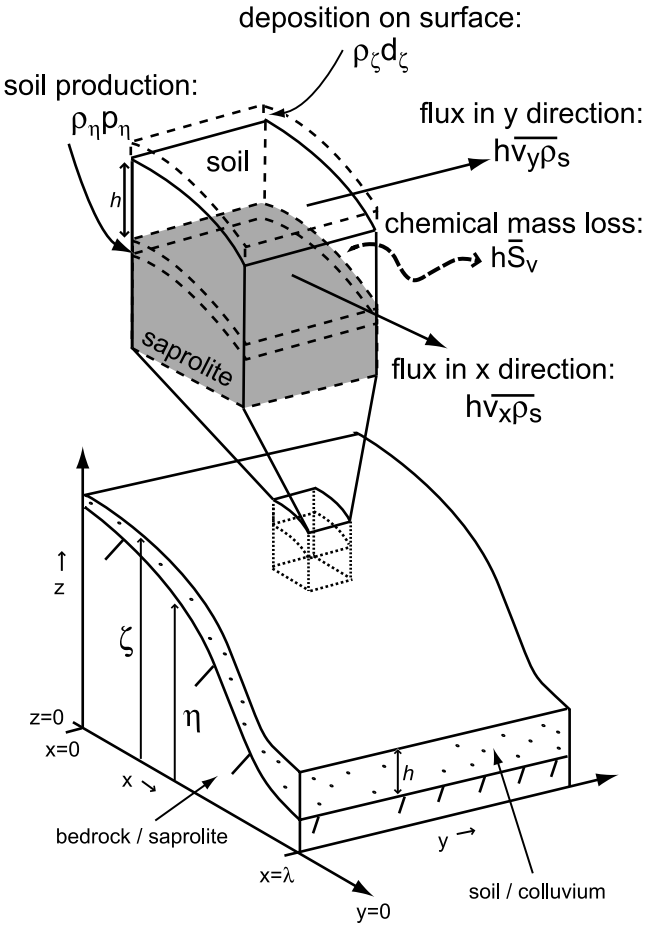

Figure 1. Schematic of the two-dimensional hillslope.

velocity of the sediment, v_z, does not appear in equation (1) because it has been eliminated by depth integration). If particle motion extends to the base of the soil as defined in a pedological sense, such that η coincides with the soil-bedrock interface, then p_η is the rate of soil production associated with the conversion of bedrock to soil. This is analogous to the production term described by *Kirkby* [1971] and examined empirically using cosmogenic isotopes [e.g., *Heimsath et al.*, 1997; *Riebe et al.*, 2003; *Small et al.*, 1999]. It is important to note that the production term does not include any mass losses due to chemical weathering; these mass losses are subsumed in the term S_v.

2.2. Conservation of a Soil Phase

[10] We now consider conservation of mass for constituent soil phases for the general framework outlined in equation (1). A phase is defined as any identifiable and unique portion of the soil (e.g., specific minerals or assemblages of minerals). In a given soil sample, the total mass of the sample is thus the sum of the masses of all the soil phases:

$$m_{tot} = \sum_{i=1}^{N} m_i, \tag{3}$$

where m_i is the mass of phase i (M), m_{tot} is the total mass in the sample (M), and N is the number of phases. The concentration by mass of phase i, c_i (dimensionless), is

$$c_i = \frac{m_i}{m_{tot}}. \tag{4}$$

Summing the concentrations by mass gives

$$\sum_{i=1}^{N} c_i = 1. \tag{5}$$

The mass of a soil phase per unit volume is

$$\frac{m_i}{V} = \frac{m_i}{m_{tot}} \frac{m_{tot}}{V} = c_i \rho_s, \tag{6}$$

where V (L^3) is a unit volume. In a control element with a surface area A (L^2), a volume V, and a vector normal to the surface $\mathbf{n}$ (L), the conservation of mass of a soil phase is described by

$$\int_V \frac{\partial}{\partial t}(c_i \rho_s) \mathrm{d}V + \int_A (\mathbf{v_i} c_i \rho_s) \cdot \mathbf{n} \, \mathrm{d}A - \int_V S_i \mathrm{d}V = 0, \tag{7}$$

where $\mathbf{v_i}$ ($L\ T^{-1}$) is the velocity vector of phase i ($\mathbf{v_i} = v_{ix}\hat{i} + v_{iy}\hat{j} + v_{iz}\hat{k}$ where $\hat{i}$, $\hat{j}$, and $\hat{k}$ are unit vectors in the x, y, and z directions, respectively, and v_{ix}, v_{iy}, v_{iz} are the respective components of the phase velocity) and S_i ($M\ L^{-3}\ T^{-1}$) is the rate of mass loss or gain of phase i per unit volume due to chemical or biological processes. The rates of the mass loss of each phase per unit volume add up to the total mass loss rate per unit volume:

$$\sum_{i=1}^{N} S_i = S_v. \tag{8}$$

[11] In order to develop a general equation of mass conservation for phase i, the method of *Mudd and Furbish* [2004] and *Paola and Voller* [2005] is used, in which equation (7) is first integrated over the control element and then depth integrated through the soil column. Kinematic boundary conditions are applied at $z = \zeta$ and $z = \eta$ [e.g., *Mudd and Furbish*, 2004; *Paola and Voller*, 2005], and it is assumed that the velocity of phase i at the boundaries is the same as the average velocity of the bulk soil. This results in a general statement of mass conservation for phase i:

$$\frac{\partial}{\partial t}(h\overline{c_i \rho_s}) + \frac{\partial}{\partial x}(h\overline{v_{ix} c_i \rho_s}) + \frac{\partial}{\partial y}\left(h\overline{v_{iy} c_i \rho_s}\right) - h\bar{S}_i - c_{i\zeta}\rho_\zeta d_\zeta - c_{i\eta}\rho_r p_\eta = 0, \tag{9}$$

where the overbars represent a depth-averaged quantity, $c_{i\zeta}$ is the concentration of phase i in material deposited at the surface of the soil (dimensionless), and $c_{i\eta}$ is the concentration of phase i at the soil-saprolite boundary (dimensionless). The first term in equation (9) is the change with respect to time of the mass of phase i in a column of soil. The second and third terms are the mass fluxes of phase i in the x and y directions, respectively. The fourth

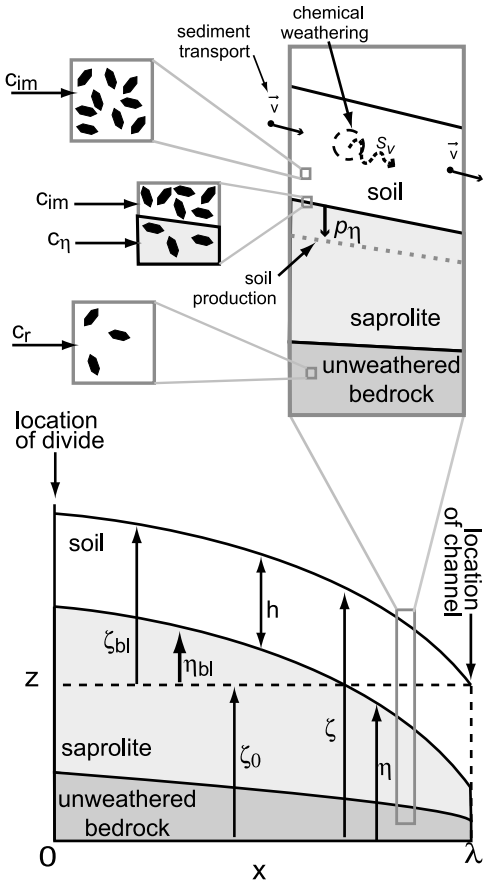

Figure 2. Schematic of the one-dimensional hillslope. The black particles represent the immobile phase in the bedrock, saprolite, and soil.

term is the rate of mass of phase i lost or gained because of chemical or biological processes (e.g., weathering of minerals, deposition of plant material). The last two terms are rate of mass of phase i lost or gained because of deposition of material on the surface of the soil or production of soil at the soil-saprolite boundary.

[12] Equations (1) and (9) are the most general forms of the equations that describe the depth-integrated conservation of mass for the soil profile and for a given soil phase i, respectively. They have a number of independent variables and therefore must be closed with simplifying assumptions and additional constitutive equations before they can be solved analytically or with numerical models.

3. A One-Dimensional, Two-Phase Model of Hillslope Soil Weathering and Transport

[13] We now develop a two-phase soil weathering and transport model that consists of a chemically mobile phase with concentration c_m and a chemically immobile phase with concentration c_{im}. All mass lost because of chemical weathering is removed from the mobile phase:

$$\overline{S}_{im} = 0, \tag{10a}$$

$$\overline{S}_m = \overline{S}_v. \tag{10b}$$

For example, an immobile phase commonly used in geochemical mass balance studies [e.g., *Brimhall et al.*, 1992] is the mineral zircon, which is highly insoluble compared to other rock forming minerals. If an element (e.g., zirconium) only occurs in the immobile mineral (e.g., zircon), then the elemental concentration may be substituted for the mineral concentration. In this two-phase system, if the concentration of the immobile phase is known, then the concentration of the mobile phase is also known (equation (5)) and we only need a conservation statement for one of the soil phases. Here we solve the governing equations for the immobile phase. We conceptualize the hillslope as having three layers (Figure 2): the soil, a saprolite layer from which the soil is produced, and a layer of unweathered bedrock. The concentration of the immobile element in these three layers is denoted by c_{im} in the soil, c_η at the soil-saprolite boundary, and c_r in the unweathered bedrock.

3.1. Simplifying Assumptions

[14] We begin by reducing the system to a one dimensional hillslope and assuming that deposition at the surface of the soil is zero ($d_\zeta = 0$). We also assume that the soil is well mixed such that products that are depth integrated can be assumed to be the products of depth-integrated quantities (e.g., $\overline{v_{ix} c_i \rho_s} \cong \overline{v}_{ix}\ \overline{c}_i\ \overline{\rho}_s$). Additionally, it is assumed that there is no sorting, such that the velocity of any given phase is the same as the bulk soil velocity ($v_{ix} = v_x$ throughout the soil column). It is also assumed that sediment at the soil-saprolite interface does not have horizontal velocities ($v_x|_{z=\eta} = v_y|_{z=\eta} = 0$).

[15] The rate of production of mobile soil from saprolite has been found to decrease with soil thickness (h) at some field locations [e.g., *Heimsath et al.*, 1997]:

$$p_\eta = W_0 e^{-\frac{h}{\gamma}}, \tag{11}$$

where W_0 ($L\ T^{-1}$) is the rate of soil production as the soil thickness approaches zero and γ (L) is a length scale that characterizes the rate of decline in the soil production rate with increasing soil thickness. We also assume that the depth-integrated density of the soil is homogenous in the x and y directions. It has been suggested that the soil production function in many locations is peaked, with a maximum value at an intermediate soil depth [e.g., *Anderson*, 2002; *Carson and Kirkby*, 1972; *Gilbert*, 1909; *Wilkinson et al.*, 2005]. Here, however, we assume that the soils of our modeled hillslopes are thick enough such that they lie on the portion of the soil production function where the production rate decreases with increasing soil thickness.

3.2. Flux Laws

[16] A number of authors have presented constitutive equations for sediment flux [e.g., *Anderson*, 2002; *Andrews and Bucknam*, 1987; *Culling*, 1963; *Gabet*, 2000; *Gabet et al.*, 2003; *Kirkby*, 1967; *Roering et al.*, 1999; *Roering*, 2004]. A general equation for describing sediment flux, ϕ, is

$$\phi = h\overline{v}_x \tag{12}$$

where ϕ has units $L^3\ L^{-1}\ T^{-1}$. The form of ϕ may vary depending on the site. We present two flux laws commonly

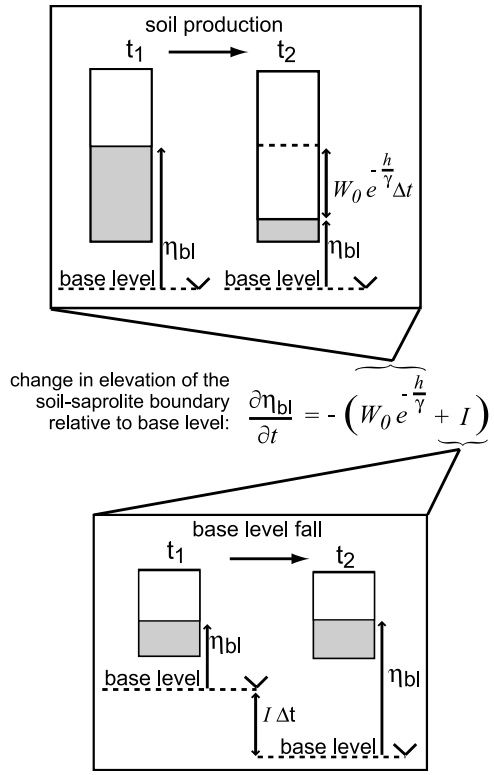

Figure 3. Schematic showing mechanisms for changing the elevation of the soil-saprolite boundary relative to base level.

used in hillslope studies, the first where sediment flux is linearly proportional to slope (equation (13a)), and the second where sediment flux increases nonlinearly as the soil surfaces approaches a critical gradient (equation (13b)):

$$\phi = -D\frac{\partial \zeta}{\partial x}, \tag{13a}$$

$$\phi = -D\frac{\partial \zeta}{\partial x}\left(1 - \left[\frac{1}{S_c}\left|\frac{\partial \zeta}{\partial x}\right|\right]^2\right)^{-1}, \tag{13b}$$

where D ($L^2\ T^{-1}$) is a sediment diffusivity and S_c is a critical slope (dimensionless).

3.3. Lagrangian Coordinate System

[17] Dynamic hillslope evolution is driven in part by incision at the base of the hillslope, and here we impose this external forcing on our modeled hillslope. We use a coordinate system in which the elevation of the soil surface (ζ) and the elevation of the soil-saprolite boundary (η) are measured relative to the local base level, which is the elevation at the base of the hillslope:

$$\zeta_{bl} = \zeta - \zeta_0, \tag{14a}$$

$$\eta_{bl} = \eta - \zeta_0, \tag{14b}$$

where the subscript *bl* indicates an elevation relative to base level and ζ_0 is the elevation of local base level, taken here to be the absolute elevation at the base of the hillslope (Figure 2). For hillslopes responding to transient incision rates, the time derivatives of both the elevation of the soil surface (ζ) and the elevation of the base of soil-saprolite boundary (η) must contain a base level lowering term ($\partial\zeta_0/\partial t$). This term is the incision or deposition rate at the lower boundary of the hillslope, which we call I ($L\ T^{-1}$). If there is a river that is incising through bedrock at the base of the hillslope, I will be negative. If the base of the hillslope is a colluvial hollow that is filling with sediment, I will be positive.

3.4. The Governing Equations for a Hillslope Soil Composed of Two Phases

[18] Noting that the soil thickness $h = \zeta - \eta = \zeta_{bl} - \eta_{bl}$, the governing equations for a one-dimensional, two-phase hillslope may be stated as

$$\frac{\partial \eta_{bl}}{\partial t} = -\left(W_0 e^{-\frac{h}{\gamma}} + I\right), \tag{15}$$

$$\frac{\partial \zeta_{bl}}{\partial t} = -\frac{\partial \phi}{\partial x} + \frac{h}{\overline{\rho}_s}\overline{S}_v - \left(1 - \frac{\rho_\eta}{\overline{\rho}_s}\right)W_0 e^{-\frac{h}{\gamma}} - I, \tag{16}$$

and

$$\frac{\partial}{\partial t}(h\overline{c}_{im}) = -\frac{\partial}{\partial x}(\phi\overline{c}_{im}) + \frac{\rho_\eta}{\overline{\rho}_s}c_{\eta im}W_0 e^{-\frac{h}{\gamma}}. \tag{17}$$

[19] Equation (15) describes the rate of lowering of the boundary between soil and saprolite relative to base level (Figure 3). Soil production (the first term to the right of the equality) will lower this boundary, whereas channel incision (the second term) will increase the elevation of the boundary relative to base level (e.g., incision causes the difference between the elevation of the soil-saprolite boundary and the channel to grow). Equation (16) describes the evolution of the elevation of the soil surface through time (Figure 4). The first term to the right of the equality in equation (16) is the rate of change of the elevation of the soil surface due to the divergence of sediment flux, the second term is the rate of change of the elevation of the soil surface due to chemical weathering, and the third term is the rate of change of the elevation of the soil surface due to expansion or contraction of the soil when it is converted from saprolite to soil. The last term is the rate of change of the elevation of the soil surface due to incision and appears because the elevation of the soil surface is measured relative to local base level. Equation (17) describes the change in time of the relative depth of the immobile phase (e.g., if a soil column is 1.0 m thick, and the concentration of the immobile phase in this column is 0.1, then the relative depth of the immobile phase is 0.1 m). The first term to the right of the equality in equation (17) describes changes in the relative depth of the immobile phase due to sediment transport, and the second term describes changes in the relative depth of the immobile phase due to soil production.

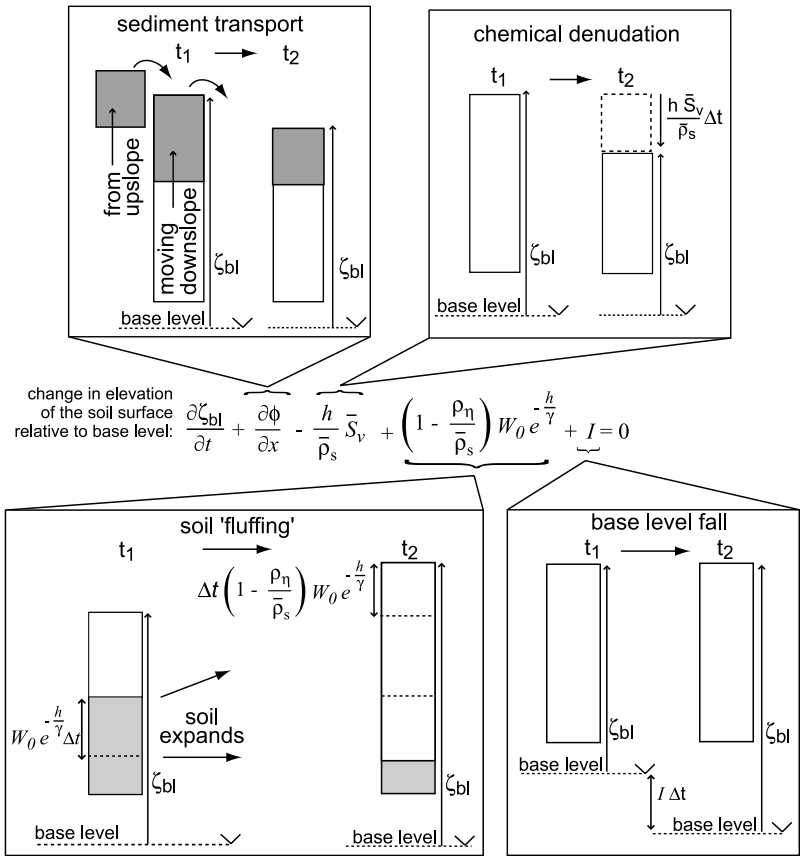

Figure 4. Schematic showing mechanisms for changing the elevation of the soil surface relative to base level.

[20] Equations (15), (16), and (17) may be combined to form an equation that describes the possible mechanisms for enriching or depleting the concentration of the immobile element in the soil (Figure 5):

$$h\frac{\partial \overline{c}_{im}}{\partial t} = -\phi\frac{\partial \overline{c}_{im}}{\partial x} - \overline{c}_{im}\frac{h\overline{S}_v}{\overline{\rho}_s} - \frac{\rho_\eta}{\overline{\rho}_s}\left(\overline{c}_{im} - c_{\eta im}\right)W_0 e^{-\frac{h}{\gamma}}. \qquad (18)$$

The concentration of the immobile phase at some point on the hillslope may be affected by the transport of sediment in areas of spatial concentration gradients, which is described by the second term in equation (18). Thinning of soil by chemical dissolution will lead to an increase in the concentration of an immobile element (third term of equation (18)). The fourth term of equation (18) describes the enrichment or dilution of the concentration of the immobile phase due to soil production.

3.5. Nondimensionalization and Scaling

[21] The number of parameters in the system described by equations (15), (16), and (17) may be reduced by nondimensionalizing the system. The length scales are nondimensionalized with either the length of the hillslope, λ (L), or the decay depth of the soil production function γ (see equation (11)):

$$\hat{x} = \frac{x}{\lambda}, \quad \hat{\zeta} = \frac{\zeta_{bl}}{\lambda}, \quad \hat{\eta} = \frac{\eta_{bl}}{\lambda}, \quad \hat{h} = \frac{h}{\gamma}, \qquad (19)$$

where dimensionless quantities are denoted with the carats. A length-scale ratio (dimensionless) is defined as

$$\theta_L = \frac{\lambda}{\gamma}. \qquad (20)$$

We also define two timescales. The first timescale (T_D) is based on the relaxation time hillslope experiencing diffusion-like sediment transport [e.g., *Fernandes and Dietrich*, 1997; *Furbish and Fagherazzi*, 2001; *Jyotsna and Haff*, 1997; *Roering et al.*, 2001], and the second (T_P) is formed with soil production parameters:

$$T_D = \frac{\lambda^2}{D}, \qquad T_p = \frac{\gamma}{W_0}, \qquad (21)$$

where we name T_D the diffusive timescale and T_P the production timescale. The diffusive timescale will range from tens of thousands to tens of millions of years [*Mudd and Furbish*, 2004]. Studies of soil or regolith production have found values of W_0 that range from approximately 1×10^{-5} m yr^{-1} to 2.5×10^{-4} m yr^{-1} and values of γ that range from approximately 0.25 m to 0.5 m [*Heimsath et al.* 1999, 2000, 2001; *Small et al.*, 1999]. This gives production timescales ranging from thousands to tens of thousands of years. We scale time, the depth-integrated mass loss due to chemical weathering per unit volume per

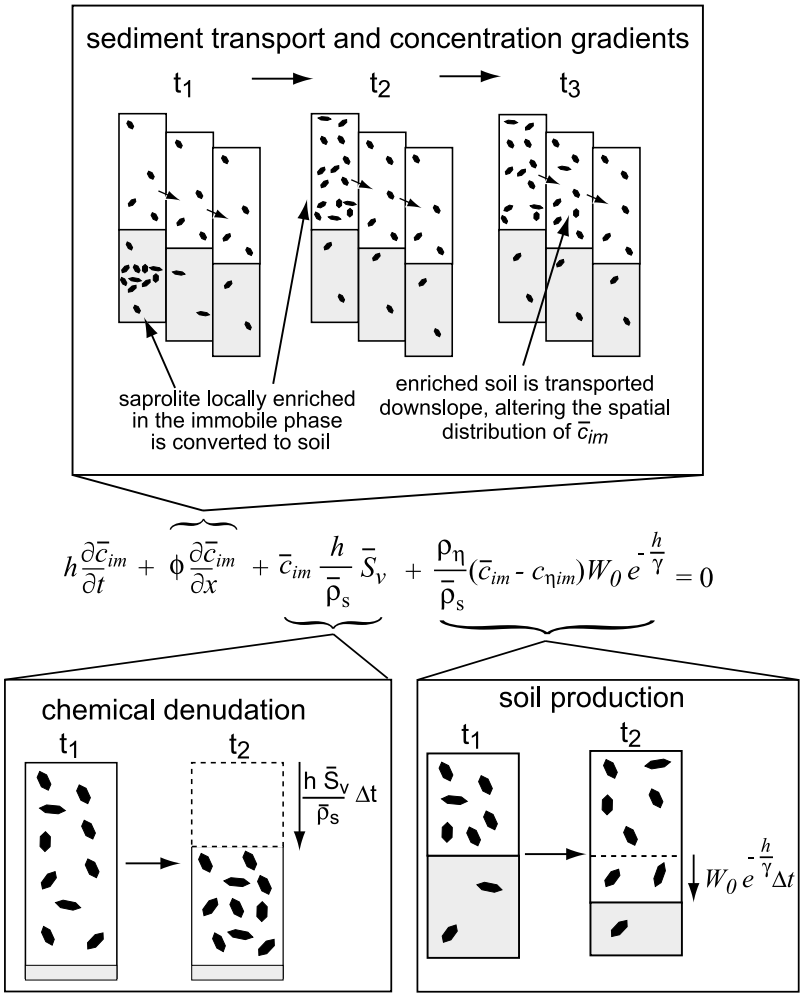

Figure 5. Schematic of the mechanisms that change the concentration of the chemically immobile phase within the soil layer.

unit time, and the base level lowering rate by the two timescales:

$$\hat{t} = \frac{t}{T_D}, \quad \hat{S} = \frac{T_P}{\bar{\rho}_s}\bar{S}_v, \quad \hat{I} = \frac{T_P}{\gamma}I. \tag{22}$$

Sediment flux is scaled by the diffusivity:

$$\hat{\phi} = -\frac{\phi}{D}. \tag{23}$$

We define a diffusive to production timescale ratio (dimensionless) as

$$\theta_t = \frac{T_D}{T_P} = \frac{\lambda^2 W_0}{D\gamma} \tag{24}$$

and a soil to parent material density ratio (dimensionless) as

$$\tau_d = \frac{\rho_\eta}{\bar{\rho}_s}. \tag{25}$$

The dimensionless concentration of the immobile phase is scaled by the concentration of this phase in the bedrock:

$$\hat{c} = \frac{\bar{c}_{im}}{c_r}, \qquad \hat{c}_\eta = \frac{c_{\eta im}}{c_r}. \tag{26}$$

If chemical weathering is occurring on the hillslope, the concentration of the immobile phase in the soil will become enriched relative to the parent material (Figure 5), so the dimensionless concentration of the immobile phase in the soil ($\hat{c}$) and at the base of the soil ($\hat{c}_\eta$) represent enrichment ratios. The subscript *im* is dropped from the dimensionless concentrations because we are solving for the concentration of the immobile phase.

[22] Inserting equations (19)–(26) into equations (15), (16), and (17) results in

$$\frac{\partial \hat{\eta}}{\partial \hat{t}} = -\frac{\theta_t}{\theta_L}\left(e^{-\hat{h}} + \hat{I}\right), \tag{27}$$

$$\frac{\partial \hat{\zeta}}{\partial \hat{t}} = \frac{\partial \hat{\phi}}{\partial \hat{x}} + \frac{\theta_t}{\theta_L}\left[\hat{h}\hat{S} - (1-\tau_d)e^{-\hat{h}} - \hat{I}\right], \tag{28}$$

and

$$\frac{\partial}{\partial \hat{t}}\left(\hat{h}\hat{c}\right) = \theta_L \frac{\partial}{\partial \hat{x}}\left(\hat{\phi}\hat{c}\right) + \theta_t \hat{c}_\eta \tau_d e^{-\hat{h}}. \quad (29)$$

The large number of model parameters in equations (19)–(26), namely W_0, γ, λ, D, $\overline{\rho}_s$, and ρ_η, are subsumed into three dimensionless groups (θ_t, θ_L, and τ_d) in the dimensionless equations (27)–(29). A single choice of a given value for any of the dimensionless groups can represent numerous hillslopes when the dimensionless governing equations are used.

4. On the Use of the Two-Phase Hillslope Model of Weathering and Transport

[23] Equations (27)–(29) may be used to explore the impact of the relative magnitude of chemical and mechanical denudation on hillslopes. Several recent studies [*Riebe et al.*, 2001, 2003, 2004a, 2004b] have suggested that if the enrichment of an immobile element and the total denudation rate (the sum of the chemical and mechanical denudation rates) are known, then the relative proportion of chemical to mechanical weathering may be determined using the relationship:

$$r_{ca} = r_T\left(1 - \frac{c_\eta}{c_{im}}\right), \quad (30)$$

where r_{ca} ($L\ T^{-1}$) is the apparent denudation rate due to chemical weathering measured by the technique of *Riebe et al.* [2001] and r_T ($L\ T^{-1}$) is the total denudation rate. If the soil production rate is steady in time then the total denudation rate is the rate of conversion of saprolite to soil ($r_T = p_\eta$) and can be determined by using cosmogenic radionuclides collected at the soil-saprolite interface [e.g., *Heimsath et al.*, 1997; *Small et al.*, 1997]. The soil production is a function of the soil depth, so the assumption that the soil production rate is steady in time also implies that soil thickness is assumed to be steady in time. *Riebe et al.* [2001] also defined a chemical depletion fraction, or CDF, which can be directly related to the enrichment fraction:

$$CDF = \left(1 - \frac{\hat{c}_\eta}{\hat{c}}\right). \quad (31)$$

The CDF has been used by *Riebe et al.* [2001, 2003, 2004a, 2004b] to estimate the fraction of the total denudation that is occurring through chemical processes (which we call the denudation ratio [e.g., *Mudd and Furbish*, 2004]), but this estimate matches the true fraction of denudation occurring through chemical processes only under certain conditions [*Riebe et al.*, 2001, appendix]. The first condition is in the case where soil experiences no sediment fluxes from upslope (e.g., a soil on a flat terrace or at a drainage divide). In that case, the apparent chemical denudation rate is equal to the actual chemical denudation rate, r_c, at that location. If there is downslope sediment transport, the chemical depletion fraction only yields the exact fraction of denudation occurring through chemical processes if the following two conditions are met: (1) the chemical composition of the parent material from which the soil is entrained is spatially homogenous and (2) the chemical denudation rate does not vary in space. *Riebe et al.* [2001, 2004a] sampled extensively in watersheds in the Sierra Nevada (various sites) and Puerto Rico (Rio Icaros watershed) and found that there were only weak variations in the chemical composition of the soils and parent material in space. At the Rio Icaros watershed in Puerto Rico, intense weathering at the soil-bedrock boundary leaves the saprolite, from which the soil is formed, almost completely devoid of minerals such as plagioclase and hornblende [*White et al.*, 1998], such that the parent material of the soil is effectively homogenous in space.

[24] Many hillslope soils, however, have chemical compositions that vary strongly in space [e.g., *Birkeland*, 1999]. The spatial distribution of the chemical composition of the soil, including the immobile elements, depends on the spatial variation in chemical denudation rates in the soil, the transport of material with differing age and composition from upslope, and the spatial variation in parent material composition (Figure 5). To calculate the basin-averaged chemical denudation rate, R_c, one must integrate the local denudation rate, r_c, over the entire basin (or over the one-dimensional transect used here, Figure 6).

[25] It should be noted that the denudation rates discussed here refer to denudation within the soil profile only, and does not include the mass lost to weathering processes within the saprolite. Also, all denudation rates in this contribution refer to rock equivalent units, for example $r_c \cdot \Delta t$ is the thickness of rock lost in time Δt from within the soil, but the thickness of soil lost will be greater by the ratio of the density of the parent material to the density of the soil, τ_d. The local rate of chemical denudation is defined by

$$r_c = -\frac{h\overline{S}_v}{\overline{\rho}_s \tau_d}. \quad (32)$$

We define both a local chemical denudation ratio, $\Theta_{dl} = r_c/r_T$, which is a function of position, and an integrated watershed denudation ratio $\theta_d = R_c/R_T$, that takes one value for a given hillslope (Figure 6c). These are the ratios of the chemical denudation rate to the total denudation rate. For example, if $\theta_d = 0.5$, then half of all the soil produced on a hillslope is denuded chemically, whereas if $\Theta_{dl} = 0.5$, then the local lowering rate due to chemical denudation in rock equivalent units ($h\overline{S}_v/\rho_\eta = h\overline{S}_v/\tau_d\overline{\rho}_s$) is half of the local rate of soil production.

[26] The apparent local rate of chemical denudation, r_{ca}, diverges from the actual local rate of chemical denudation, r_c, for several reasons. We explore two important mechanisms that lead to apparent chemical denudation rates that differ from the actual chemical denudation rates that are manifested in the presence of downslope sediment transport. The reasons that we explore are spatial variations in the mass loss rate due to chemical weathering (S_v) and spatial variations in the enrichment of the immobile phase at the soil-saprolite boundary (c_η). These mechanisms are studied using the simple but illustrative case of a steady state hillslope, which allows for analytic solution of equations

(27)–(29). The effect of transient incision or deposition rates are also explored using nonsteady state models.

4.1. Steady State Solution of the Two-Phase Hillslope Model

[27] For a hillslope that is in steady state, the time derivatives in equations (27)–(29) vanish. The governing equations then become

$$-e^{-\hat{h}} = \hat{I}, \tag{33}$$

$$\frac{\partial \hat{\phi}}{\partial \hat{x}} = \frac{\theta_t}{\theta_L}\left(\tau_d \hat{I} - \hat{h}\hat{S}\right), \tag{34}$$

$$\hat{c}\frac{\partial \hat{\phi}}{\partial \hat{x}} + \hat{\phi}\frac{\partial \hat{c}}{\partial \hat{x}} = \frac{\theta_t}{\theta_L}\hat{c}_\eta \tau_d \hat{I}. \tag{35}$$

The dimensionless incision rate, $\hat{I}$, is constant in time, such that the dimensionless soil depth is also constant in time and space by equation (33). To close the system, we define the spatial distribution of dimensionless mass loss rate due to chemical weathering, $\hat{S}$, and the spatial distribution of the enrichment of the immobile phase at the soil-saprolite boundary, $\hat{c}_\eta$. Although the sediment flux law (e.g., equation (13a) or (13b)) influences the surface topography ($\hat{\zeta}$), slope ($\partial\hat{\zeta}/\partial\hat{x}$) and curvature ($\partial^2\hat{\zeta}/\partial\hat{x}^2$), it does not influence the spatial distribution of the enrichment of the immobile phase on the hillslope ($\hat{c}$). This is shown in the solution to equation (35) presented later in this section. For the analysis of the steady state case the simplest possible spatial variations of the dimensionless mass loss rate due to chemical weathering, $\hat{S}$, and the dimensionless concentration of the immobile phase at the base of the soil, $\hat{c}_\eta$, are assumed; they are approximated by linear functions (we consider more complex spatial variations in Appendix A):

$$\hat{S} = \chi(1-\hat{x}) + \hat{S}_{divide}, \tag{36}$$

$$\hat{c}_\eta = \sigma(1-\hat{x}) + \hat{c}_{\eta divide}, \tag{37}$$

where χ and σ (dimensionless) describe the variation of $\hat{S}$ and $\hat{c}_\eta$ as a function of space and the subscript *divide* indicates the value of the parameter at the hillslope divide. Recall that $\hat{S}$ is negative if mass is lost to chemical weathering, so if χ is negative the dissolution rate increases downslope. If σ is positive, then the enrichment of the immobile phase at the soil-saprolite boundary increases downslope. No flux passes through the divide ($\hat{\phi}|_{\hat{x}=1} = 0$), whose location is at $\hat{x} = 1$. At the divide, the enrichment of the immobile phase in the soil is set by the ratio of chemical to total denudation at the divide and the enrichment of the immobile element at the soil-saprolite boundary at the divide:

$$\hat{c}|_{\hat{x}=1} = \hat{c}_{\eta divide}\left(1 - \frac{\hat{h}\hat{S}_{divide}}{\hat{I}\tau_d}\right)^{-1}. \tag{38}$$

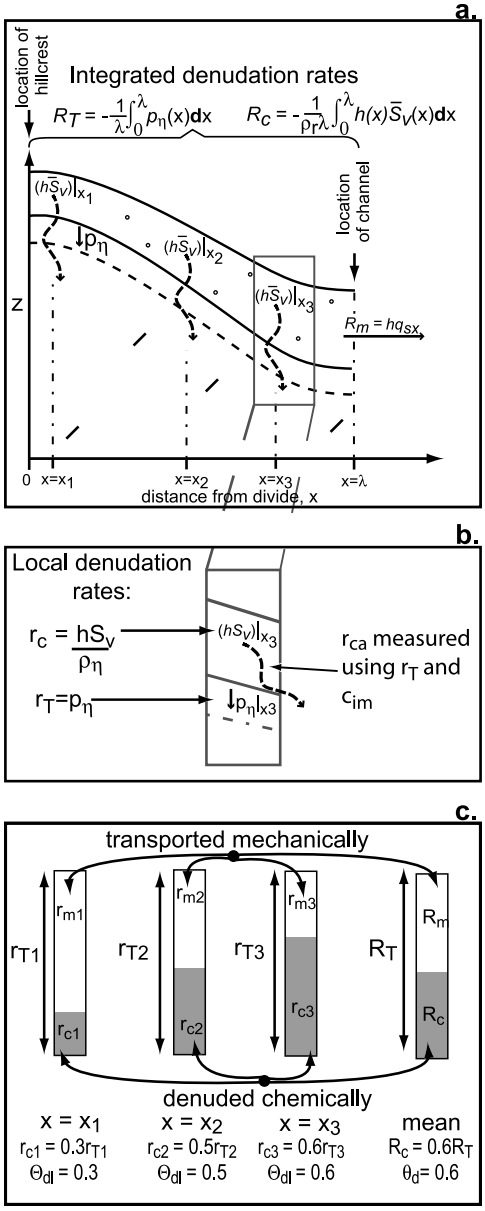

Figure 6. Schematic of the (a) integrated denudation rates and (b) local denudation rates. (c) Spatial variations in the local denudation ratio and the integrated denudation ratio.

[28] Inserting equation (37) into equation (35) yields an ordinary differential equation whose solution, given the constant boundary condition described by equation (38) and the no flux condition at the divide, is:

$$\hat{c} = \frac{\theta_t \hat{I}\tau_d}{2\,\theta_L}\frac{(\hat{x}-1)\left[2\,\hat{c}_{\eta divide} + \sigma(1-\hat{x})\right]}{2\hat{\phi}}. \tag{39}$$

Similarly, the flux as a function of space may be solved by inserting equation (36) into equation (34) and integrating:

$$\hat{\phi} = \frac{\theta_t}{2\,\theta_L}(\hat{x}-1)\left[2\,\hat{I}\tau_d - \hat{h}\left(\chi(\hat{x}-1) + 2\hat{S}_{divide}\right)\right]. \tag{40}$$

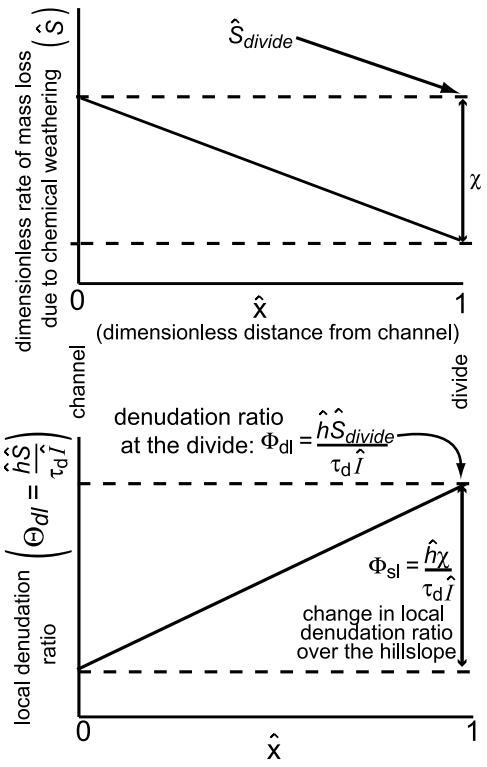

Figure 7. Schematic showing (top) linear variation in space of the dimensionless mass loss rate due to chemical weathering ($\hat{S}$) and (bottom) its relationship to the spatial variation in the local denudation ratio (Θ_{dl}).

Equations (39) and (40) may be combined and simplified to yield the steady state solution for the enrichment of the immobile phase in the soil:

$$\hat{c} = \frac{\sigma(1-\hat{x}) + 2\,\hat{c}_{\eta divide}}{2(1-\Phi_{dl}) + \Phi_{sl}(\hat{x}-1)}, \tag{41}$$

where

$$\Phi_{dl} = \frac{\hat{h}\hat{S}_{divide}}{\hat{I}\tau_d}, \qquad \Phi_{sl} = \frac{\hat{h}\chi}{\hat{I}\tau_d}. \tag{42}$$

The ratios Φ_{dl} and Φ_{sl} represent the local denudation ratio at the divide and the change in the local denudation ratio over the length of the hillslope (Figure 7). In the steady state case where $\hat{S}$ is described by equation (36) the local denudation ratio, Θ_{dl}, is

$$\Theta_{dl} = \Phi_{sl}(1-\hat{x}) + \Phi_{dl}. \tag{43}$$

If the chemical denudation rate increases downslope, then Φ_{sl} is positive. The chemical depletion fraction (CDF) may be calculated by inserting equations (37) and (41) into equation (31). Several enrichment profiles and the corresponding CDF profiles are shown in Figures 8 and 9. In Figure 8, the enrichment of the immobile phase in the soil-saprolite interface increases downslope although the local denudation ratio does not vary in space. In Figure 9, the enrichment of the immobile phase at the base of the soil, $\hat{c}_\eta$, is constant in space and the local denudation ratio increases downslope (e.g., greater chemical weathering rates downslope). If $\sigma = 0$, the chemical depletion fraction is not a

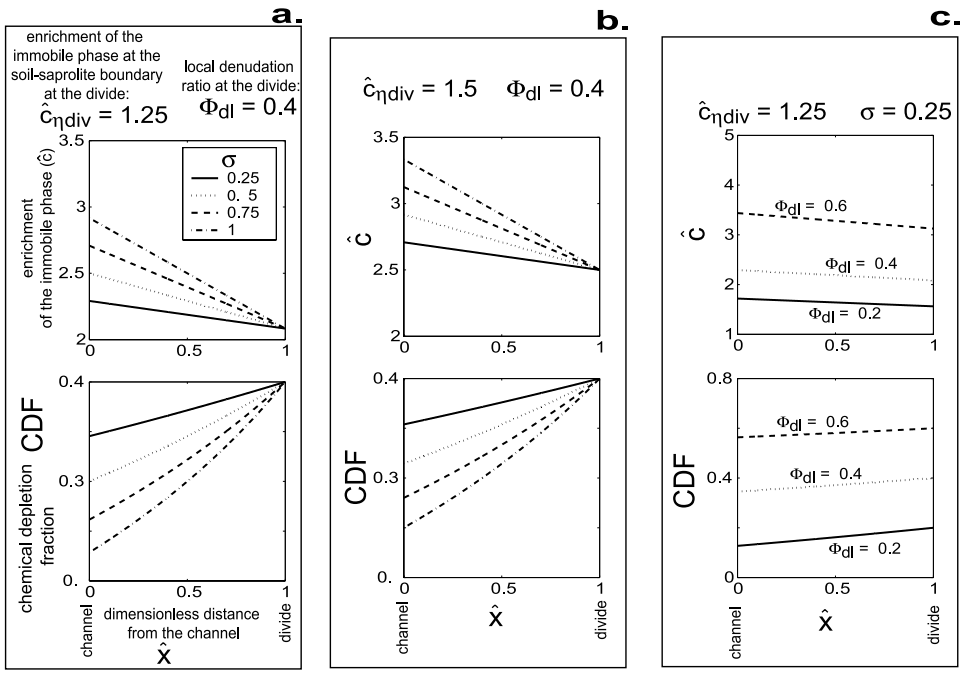

Figure 8. Plots of enrichment of the immobile phase in the soil ($\hat{c}$) and the chemical depletion fraction (CDF) for steady state solutions of the two-phase hillslope system where there is no spatial variation in the local chemical denudation rate ($\Phi_{sl} = 0$). Legend in Figure 8a applies to all plots in Figures 8a and 8b.

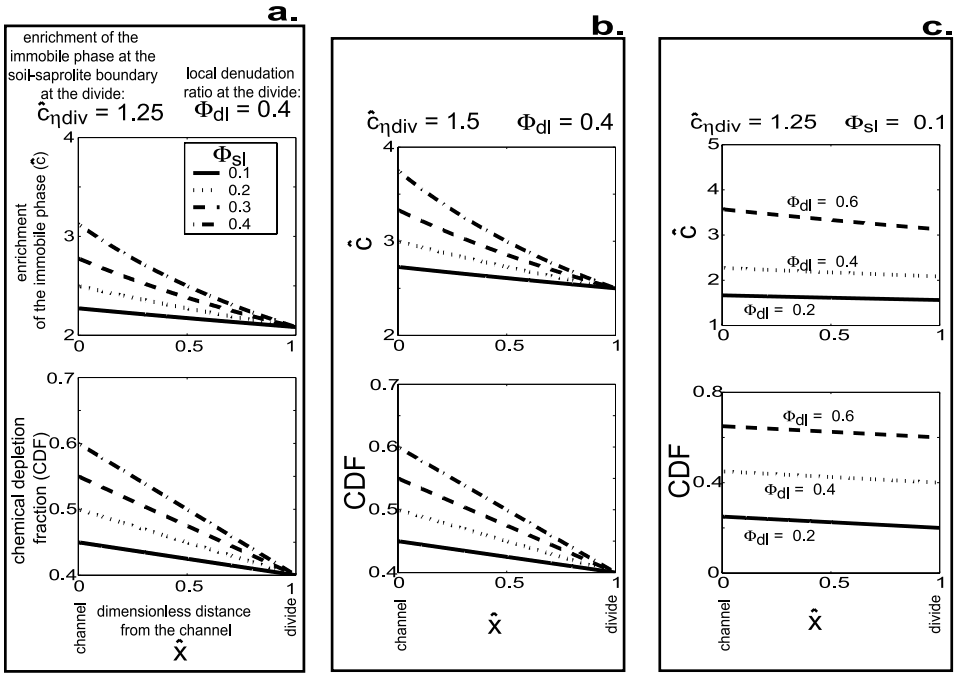

Figure 9. Plots of enrichment of the immobile phase in the soil ($\hat{c}$) and the CDF for steady state solutions of the two-phase hillslope system where there is no spatial variation in the enrichment of the immobile phase at the soil-saprolite boundary ($\sigma = 0$). Legend in Figure 9a applies to all plots in Figures 9a and 9b.

function of the enrichment of the immobile phase at the soil-saprolite boundary at the divide (the plots of the CDF in Figures 9a and 9b are identical). When the enrichment of the immobile phase at the base of the soil ($\hat{c}_\eta$) varies linearly in space, the downslope variation in the dimensionless concentration of the immobile phase in the soil ($\hat{c}$) is linear, whereas when the local denudation ratio ($_{Dl}$) varies linearly, the downslope variation in the enrichment of the immobile phase, $\hat{c}$, is nonlinear.

[29] While both of the sets of solutions represent an increase in chemical weathering downslope, with the first set having increased weathering in the saprolite, and the second having increased rate of chemical denudation in the soil, the resulting plots of the chemical depletion fraction (CDF) vary significantly. In the first set (Figure 8) the CDF decreases downslope, whereas in the second set the CDF increases downslope. The decrease in the chemical depletion fraction as one moves downslope in Figure 8 highlights the fact that on hillslopes with spatially varying enrichment ratios of the immobile phase at the soil-saprolite boundary, an estimate of the denudation ratio based on the CDF will not exactly match the true denudation ratio. In the case of Figure 8 the local denudation ratio is the same everywhere on the slope, but the CDF varies in space because soil is being transported from upslope that is less enriched in the immobile phase because of the spatial variation in the enrichment of the saprolite.

[30] The difference between the apparent denudation ratio (as quantified by the CDF) and the actual denudation ratio (set by the dimensionless mass loss rate due to chemical weathering, $\hat{S}$) may be quantified using equations (36) and (41). The fractional difference between the true local denudation ratio (Θ_{dl}) and the denudation ratio estimated by the CDF, which we call δ_l, is

$$\delta_l = \frac{\Theta_{dl} - CDF}{\Theta_{dl}}. \tag{44}$$

Figure 10 plots δ_l for the scenarios plotted in Figures 8 and 9. If the rate of weathering is increasing downslope in either the soil-saprolite interface or in the soil itself, the chemical depletion fraction will underestimate the proportion of denudation caused by chemical weathering. Increasing either σ or χ, which increases the spatial variation in the enrichment of the immobile phase in the parent material ($\hat{c}_\eta$) and the dimensionless rate of mass loss due to chemical weathering ($\hat{S}$), respectively, increases the fractional difference in estimated and actual denudation ratios. In addition, hillslopes with lower overall denudation ratios (e.g., lower Φ_{dl}) will have larger discrepancies between the actual denudation ratio and the denudation ratio as estimated by the chemical depletion fraction. Thus accounting for sediment transport and the spatial distribution of the immobile phase in the saprolite is especially important in regions with low rates of chemical denudation relative to mechanical denudation, such as, for example, in arid regions.

[31] The integrated denudation ratio, θ_d, which is the ratio between the hillslope-averaged chemical denudation rate and the total denudation rate, may be calculated by

$$\theta_d = \frac{\hat{h}}{\hat{I}\tau_d}\int_0^1 \hat{S}\mathrm{d}\hat{x} = \Phi_{dl} + \frac{\Phi_{sl}}{2} \tag{45}$$

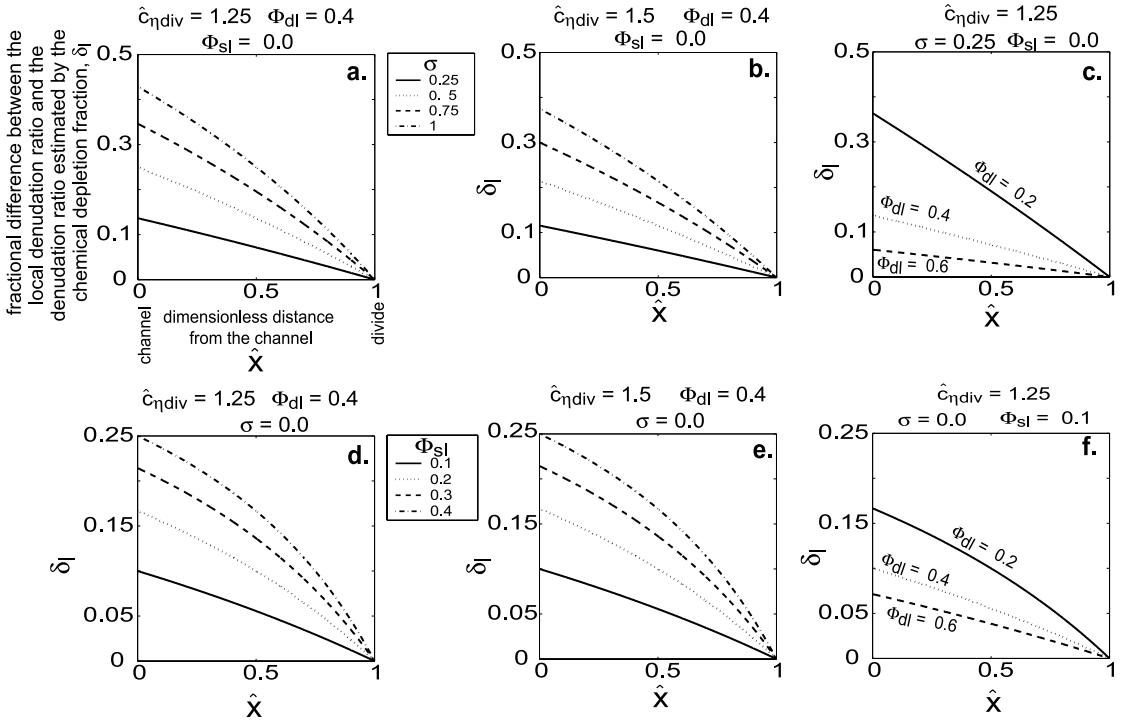

Figure 10. Normalized difference between the true local ratio of chemical to total denudation rate (Θ_{dl}) and this ratio estimated using the CDF.

If one is interested in calculating the ratio between chemical and total denudation averaged over a basin, use of the chemical depletion fraction is attractive because of its relative simplicity. Here we test the appropriateness of estimating the denudation ratio (θ_d) on hillslopes where soil is transported downslope and that have spatially heterogeneous parent material or chemical denudation rates. We consider three cases where the denudation ratio is estimated using the chemical depletion fraction measured (1) at the hillslope base ($\hat{x} = 0$), (2) midway between the hillslope base and the divide ($\hat{x} = 0.5$), and (3) at the divide ($\hat{x} = 1$). The fractional difference between the integrated denudation ratio and the denudation ratio estimated by the chemical depletion fraction, which we call δ_I, is

$$\delta_I = \frac{\theta_d - CDF}{\theta_d}. \tag{46}$$

A particular case of δ_I is when the enrichment at the soil-saprolite interface is spatially homogeneous ($\sigma = 0$). In this case, the error in the integrated denudation ratio estimated by the CDF is

$$\delta_I = \frac{\Phi_{sl}\hat{x}}{\Phi_{sl} + 2\,\Phi_{dl}}. \tag{47}$$

Equation (47) demonstrates that if the parent material has a homogenous chemical composition, the chemical depletion fraction will accurately predict the denudation ratio (θ_d, which is the ratio of the chemical denudation rate to the total denudation rate) at the base of the hillslope. On the other hand, if chemical denudation rate does not vary in space (e.g., $\Phi_{sl} = 0$), the chemical depletion fraction will accurately predict the denudation ratio at the divide. The fractional difference between the integrated denudation ratio and the denudation ratio estimated by the chemical depletion fraction (δ_I) is plotted for a range of parameter values in Figure 11. For hillslopes that experience low chemical denudation rates as a proportion of the total denudation rate (e.g., low values of Φ_{dl}), the fractional difference between the denudation ratio estimated by the chemical depletion fraction and the true denudation ratio can exceed 25%. In landscapes where chemical denudation makes up a larger proportion of the total denudation, the denudation ratio estimated by the chemical depletion fraction is expected to differ from the true denudation ratio by less than 10% if spatial variations in the chemical denudation rate are small (Figure 11).

4.2. Quantifying the Changes in the Concentration of the Immobile Phase Related to Transient Incision or Deposition

[32] If the lowering (or deposition) rate ($\hat{I}$) at the base of the hillslope changes, both the spatial distribution of the chemical denudation rate and of the enrichment of the immobile phase may be affected. Consider a hillslope that is initially at steady state with a stream at its lower boundary incising at a rate of I_0. The stream then experiences a step change in its incision rate, to a rate I. This causes soil to either be evacuated (if $I < I_0$, recall I takes a negative value for incision) or accumulate (if $I > I_0$) on the hillslope. How do chemical denudation rates respond? A simple example would be if the chemical denudation rates did not change when total denudation rates change. In this case, if the incision rate increased,

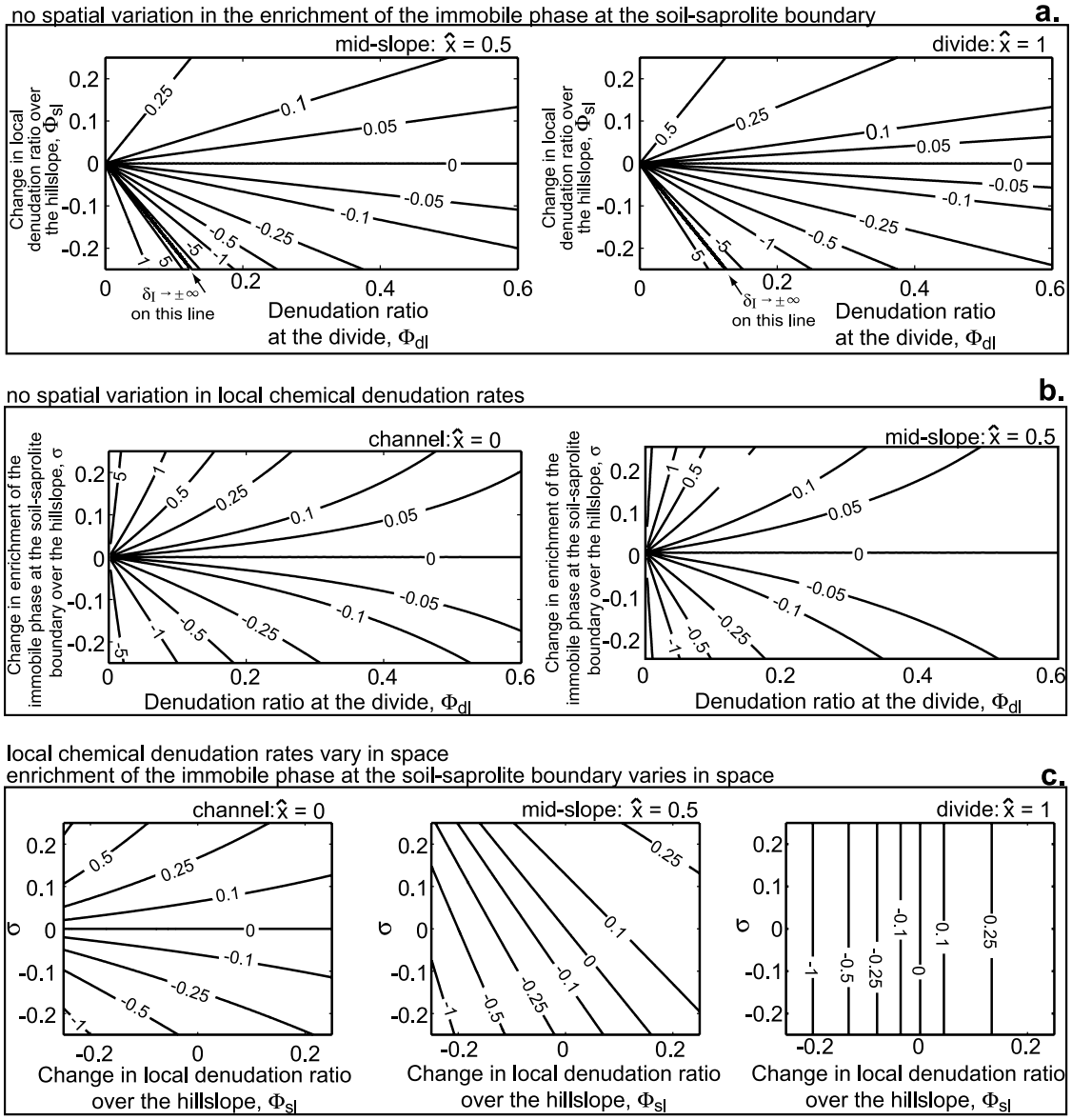

Figure 11. Contour plots of the fractional difference between the integrated denudation ratio and the denudation ratio estimated by the chemical depletion fraction (e.g., all plots show contours of $\delta_I = (\theta_d - \mathrm{CDF})/\theta_d$). In all plots the enrichment of the immobile phase at the soil-saprolite boundary at the divide is equal to 1.25 ($\hat{c}_{\eta div} = 1.25$). Each individual plot shows contours of δ_I at hillslope positions indicated above the plots (e.g., at the divide, midslope, or at the channel). (a) Hillslopes where the spatial variation in the enrichment of the immobile element at the soil-saprolite boundary does not vary in space ($\sigma = 0$). (b) Hillslopes where the spatial variation in the local denudation ratio does not vary in space ($\Phi_{sl} = 0$). (c) Hillslopes where both the local denudation ratio and the enrichment of the immobile element at the soil-saprolite boundary vary in space. In these plots the denudation ratio at the divide, Φ_{dl}, is 0.2.

then the soil would thin (see equation (15)), and because the chemical denudation rate is a product of the chemical weathering rate per unit volume and the soil thickness (see equation (32)), the chemical denudation rate would decrease as well. Conversely, under a depositional regime, the soil depth would increase and the proportion of the total denudation accounted for by chemical weathering would increase.

[33] *White and Brantley* [2003] noted that the time minerals spent in the near surface zone of weathering (or 'weathering engine') was of fundamental significance in determining the weathering rate, as fresh minerals weather many orders of magnitude faster than minerals that have been exposed to water for long periods of time. Both *Riebe et al.* [2001] and *West et al.* [2005] argue that exposure of fresh mineral surfaces in faster eroding soils is one of the causes of the trend in which landscapes that are eroding more quickly have greater rates of chemical denudation, and as we will demonstrate below, faster soil production is coupled to younger soil particles. Because soil residence

time and chemical weathering rates may be linked, spatial variations in the residence time of soil particles may also influence the spatial distribution of weathering rates.

[34] Given the potential importance of soil particles residence times in determining the rate of chemical weathering in the soil, we present here an analysis of both mean soil particle residence times and the distribution of soil particle ages. We define soil particle residence time as the time elapsed since the particle has been entrained into the mechanically active soil layer. For a "box" of hillslope soil with downslope dimension L, transverse dimension Y, and depth h, if the soil depth does not vary in time, then one way to define a mean residence time, T_R, of mass moving from bedrock into and through the soil is

$$T_R = \frac{V}{I} = \frac{\overline{\rho}_s h L Y}{\rho_r p_\eta L Y} = \frac{h}{\tau_d p_\eta}. \quad (48)$$

[35] Here, $V = hLY$ is the volume of the soil box, and $I = p_\eta LY$ is the steady (volumetric) rate of input of mass to the soil box at steady state. A number of authors [e.g., *Amundson*, 2004; *Anderson et al.*, 2002; *Small et al.* 1999] have noted this relationship between particle residence time and soil production, albeit in forms slightly different from equation (48). This mean residence time, T_R, may also be considered a "turnover time," that is, the time required to replace the volume V at an input rate I.

[36] The volumetric flux $Q(x)$ ($L^3\ T^{-1}$) (equivalent to $h\phi$) through hY at a downslope distance x is

$$Q(x) = Y \tau_d p_\eta x, \quad (49)$$

so the flux density $q(x)$ ($M\ L\ T^{-1}$) is $q(x) = \overline{\rho}_s v(x) = \overline{\rho}_s Q(x)/hY = \rho_r\ p_\eta\ x/h$, where $v = p_{?\eta}\ \tau_d\ x/h$ ($L\ T^{-1}$) is the particle velocity. Thus T_R may also be defined

$$T_R = \frac{x}{v(x)}. \quad (50)$$

It can be seen that T_R increases with x; but so does the particle velocity $v(x)$, such that T_R remains constant, as in equation (48).

[37] The coordinate x above is Eulerian. Momentarily consider x from a Lagrangian perspective, such that it denotes the position of a soil particle, in which case $v = \mathrm{d}x/\mathrm{d}t$, and

$$\frac{dx}{dt} = \frac{x}{T_R}. \quad (51)$$

Separating variables and integrating,

$$x = x_0 e^{\frac{t}{T_R}}, \quad (52)$$

where x_0 is the initial position of the particle, and $0 \leq x_0 \leq x$.

[38] For the soil box with upslope and downslope sides at $x = 0$ and $x = \lambda$, respectively, particles "entering" the soil (from bedrock) are uniformly distributed between these limits. That is, at any instant, $0 \leq x_0 \leq \lambda$ with equal probability. The probability density function $f(x_0)$ of initial positions x_0 is thus

$$f(x_0) = \frac{1}{\lambda}. \quad (53)$$

Now, let τ denote the (travel) time that it takes a particle to move from its initial position x_0 to position $x = \lambda$, and let μ_τ denote the (ensemble) average time that particles reside in the soil box before reaching λ (whence they leave the box). With these definitions we rewrite equation (52) as

$$\lambda = x_0 e^{\frac{\tau}{T_R}} \quad (54)$$

and, for reference below, rearrange this to $x_0 = \lambda \exp(-\tau/T_R)$ noting that $\partial x_0/\partial\tau = -(\lambda/T_R)\exp(-\tau/T_R)$. The probability density function $p(\tau)$ of travel times τ is defined by $p(\tau) = f(x_0)|\partial x_0/\partial\tau|$:

$$p(\tau) = \frac{1}{T_R} e^{-\frac{\tau}{T_R}}. \quad (55)$$

This is the exponential distribution with average $\mu_\tau = T_R$ and variance $\sigma^2 = T_R^2$. Thus travel times τ are "mostly" short, with the probability decreasing exponentially with increasing travel time. Whereas the starting positions x_0 are uniformly distributed between 0 and λ, speeds increase with x, so travel times are disproportionally shortened.

[39] Therefore in the steady state case no spatial variation of the mean particle residence time occurs (equation (48)), so if the mean residence time of soil particles is the dominant factor in determining the chemical denudation rate, no spatial variation in the chemical denudation rate occurs. If, however, the incision at the base of the hillslope changes, then the rate of supply of fresh particles must adjust to the new conditions, leading to spatial variations in the mean particle residence time (Figure 12) and thus spatial variations in the chemical denudation rate. If the incision rate increases (Figure 12), then in the time before the hillslope approaches its new steady state condition the soil will have a lower mean particle residence time near the base of the hillslope than at the divide. If the particle age drives the chemical denudation rate, this means that if the incision rate has recently increased, then the chemical denudation rate will increase downslope. Conversely, if the incision rate slows (Figure 12), then soil near the base of the hillslope will be older than the soil upslope, and the chemical denudation rate will decrease downslope if the mean particle residence time is the dominant factor controlling the chemical denudation rate.

5. Conclusions

[40] We have derived mass conservation equations that can be used to predict concentrations of a chemically immobile phase in a hillslope soil. Under simplifying assumptions that are relevant to certain field situations, the spatial distribution of the enrichment of this immobile phase can be solved analytically. Chemical denudation rates in a hillslope soil can be measured using the concentration of immobile elements, but the enrichment of these immobile elements is influenced by spatial variations in chemical denudation rates and the chemical composition of the material from which the soil is derived. These considera-

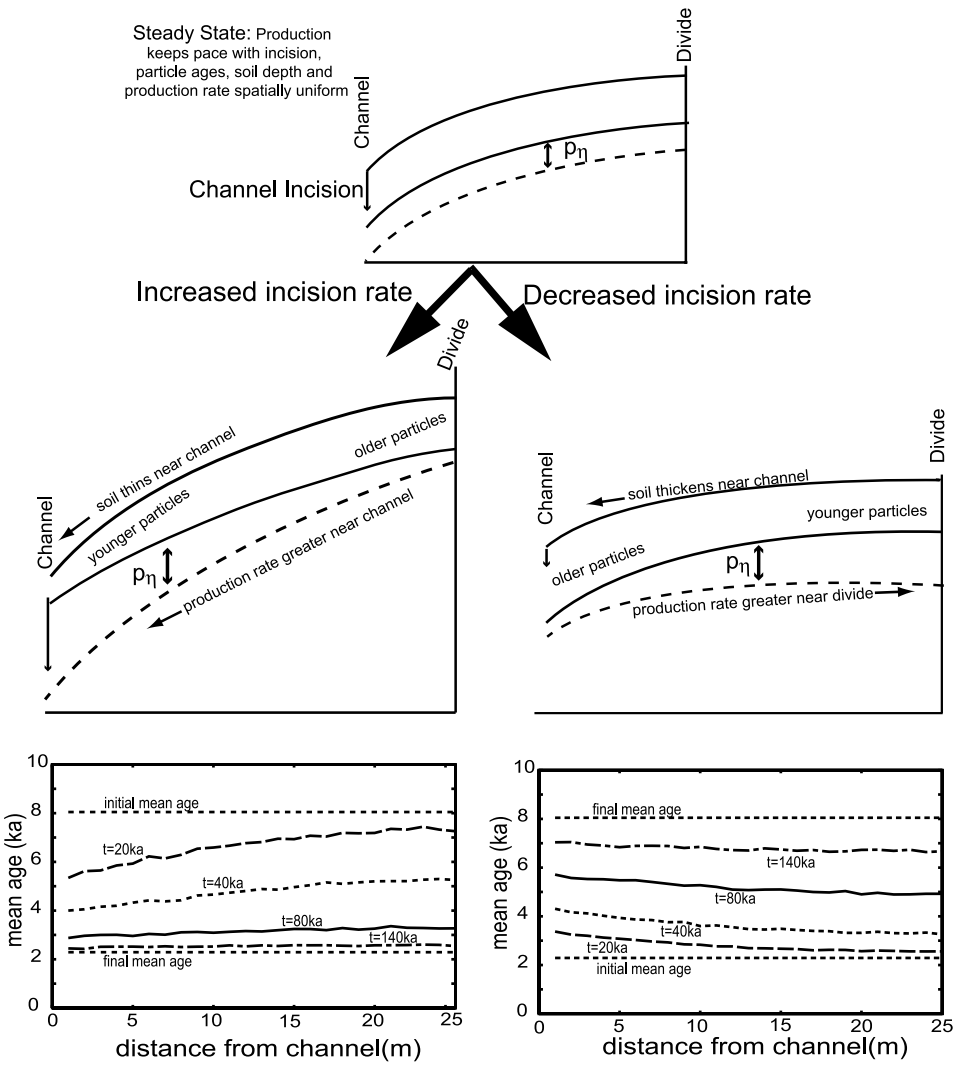

Figure 12. Diagram showing the response of a hillslope to increasing or decreasing incision rates. Bottom two figures show the calculated mean particle residence time in thousands of years as a function of position. Parameter values are $W_0 = 2.5 \times 10^{-4}$ m yr^{-1} and $\gamma = 0.5$ m, $D = 0.01$ m^2 yr^{-1}. Hillslopes are at steady state for an initial incision rate I_0 at $t = 0$, then the incision rate changes to incision rate I. The lines labeled "initial" and "final" mean particle residence times are theoretical values calculated with equation (48). Between the steady state solutions are curves of the mean particle residence time as a function of hillslope position, whose labels indicate the time elapsed after the change in incision rate. Particle residence times are calculated by a stochastic numerical model that randomly selects discrete particles to move downslope each timestep; the number of particles moving is proportional to the sediment flux. The stochastic nature of the model causes the variance about the trend in the mean ages. The divide is at $x = 25$ m. In the case of the increasing incision rate, $I_0 = 5.0 \times 10^{-5}$ m yr^{-1}, and $I = 1.0 \times 10^{-4}$ m yr^{-1}. In the case of the decreasing incision rate, $I_0 = 1.0 \times 10^{-4}$ m yr^{-1}, and $I = 5.0 \times 10^{-5}$ m yr^{-1}.

tions cloud the use of elemental depletion factors and cosmogenic nuclide-based total denudation rates [e.g., *Riebe et al.*, 2001] in identifying the relationship between physical erosion and chemical weathering where chemical denudation rates vary in space and soils are being transported downslope. Although the method of *Riebe et al.* [2001] may be inadequate in regions where the chemical denudation rate is only a small fraction of the total denudation rate, it is still useful in locations where the chemical denudation rate is a significant portion of the total denudation rate (e.g., >50%) and where sediment transport and spatial variations in chemical denudation rates only introduce small (<10%) errors in the chemical denudation rates estimated using the chemical depletion fraction of *Riebe et al.* [2001].

[41] We also present several possible responses of chemical weathering rates in the soil such as the expected distribution of particle residence times, to unsteady channel incision rates. Depositional parts of a hillslope system have locally greater particle residence times, which might be

expected to reduce the local rate of chemical denudation. These areas of deposition would also coincide with topographic hollows, however, where there is an increased likelihood of groundwater flow, which might be expected to increase weathering. Using immobile minerals to quantify weathering rates in such locations of transient deposition could allow researchers to assess the relative importance of hydrology and particle residence times on the rate of chemical weathering in hillslope soils.

Appendix A

[42] Here we offer several solutions to the steady state equations (34) and (35) based on a variety of descriptions of the spatial variation in $\hat{S}$ and $\hat{c}_\eta$. The enrichment of the immobile phase at the soil-saprolite interface may be measured in the field and then fitted. We have proposed a linear approximation in the text; here we propose three additional fits to the saprolite enrichment:

$$\hat{c}_\eta = \hat{c}_{\eta divide} e^{\frac{\hat{x}-1}{\alpha_{ce}}}, \tag{A1}$$

$$\hat{c}_\eta = \alpha_{cq}(\hat{x}-1) + \beta_{cq}(\hat{x}-1) + \hat{c}_{\eta divide}, \tag{A2}$$

$$\hat{c}_\eta = \alpha_{cp}(\hat{x}-1)^{\beta_{cp}} + \hat{c}_{\eta divide}, \tag{A3}$$

where α and β are fitting parameters, the subscript c denotes a fitting parameter for $\hat{c}_\eta$, and the subscripts e, q, and p denote parameters for the exponential, quadratic, and power law fits, respectively. The solutions to equation (35) for the three approximations given by equations (A1), (A2), and (A3) are

$$\hat{c} = \frac{\alpha_{ce}\theta_t\tau_d}{\theta_L\hat{\phi}}\left(e^{\frac{\hat{x}-1}{\alpha_{ce}}} - 1\right)\hat{c}_{\eta divide}, \tag{A4}$$

$$\hat{c} = \frac{\theta_t\hat{I}\tau_d(\hat{x}-1)}{6\theta_L\hat{\phi}}\left[6\hat{c}_{\eta divide} + \alpha_{cq}(\hat{x}-1)\left(2[\hat{x}-1] + 3\beta_{cq}\right)\right], \tag{A5}$$

$$\hat{c} = \frac{\theta_t\hat{I}\tau_d(\hat{x}-1)}{\left(1+\beta_{cp}\right)\theta_L\hat{\phi}}\left[\hat{c}_{\eta divide}\left(1+\beta_{cp}\right) + \alpha_{cp}(\hat{x}-1)^{\beta_{cp}}\right]. \tag{A6}$$

To close equations (A4)–(A6), $\hat{\phi}$ must be evaluated. To do this, a functional form of $\hat{S}$ must be proposed. Again, we provide three examples: an exponential function, a quadratic function, and a power law function:

$$\hat{S} = \hat{S}_{divide} e^{\frac{\hat{x}-1}{\alpha_{Se}}}, \tag{A7}$$

$$\hat{S} = \alpha_{Sq}(\hat{x}-1) + \beta_{Sq}(\hat{x}-1) + \hat{S}_{divide}, \tag{A8}$$

$$\hat{S} = \alpha_{Sp}(\hat{x}-1)^{\beta_{Sp}} + \hat{S}_{divide}, \tag{A9}$$

where again α and β are fitting parameters, the subscript S denotes a fitting parameter for $\hat{S}$, and the subscripts e, q, and p denote parameters for the exponential, quadratic, and power law functions, respectively. These fits lead to solutions for equation (35):

$$\hat{\phi} = \frac{\theta_t}{\theta_L}\left[\hat{S}_{divide}\left(1 - e^{\frac{\hat{x}-1}{\alpha_{Se}}}\right)\alpha_{Se}\hat{h} + (\hat{x}-1)\hat{I}\tau_d\right], \tag{A10}$$

$$\hat{\phi} = \frac{\theta_t}{6\,\theta_L}[1-\hat{x}]\left[\left(6\,\hat{S}_{divide} + [\hat{x}-1]\left[2\,\alpha_{Sq}(\hat{x}-1) + 3\beta_{Sq}\right]\right)\hat{h} - 6\,\hat{I}\tau_d\right], \tag{A11}$$

$$\hat{\phi} = \frac{(1-\hat{x})\theta_t}{\left(1+\beta_{Sp}\right)\theta_L}\left[\hat{S}_{divide}\hat{h}\left(1 + \frac{\alpha_{Sp}}{\beta_{Sp}}[\hat{x}-1]^{\beta_{Sp}} + \beta_{Sp}\right) - \left(1+\beta_{Sp}\right)\hat{I}\tau_d\right]. \tag{A12}$$

Notation

-	overbars denote depth-integrated quantities.
^	carats denote dimensionless quantities.
α	fitting parameter (see Appendix A).
β	fitting parameter (see Appendix A).
c_i	concentration of phase i (dimensionless).
c_m, c_{im}	concentration of the chemically mobile and immobile phases (dimensionless).
c_η, c_r	concentration of the immobile phase at the soil-saprolite interface and in the bedrock (dimensionless).
$\hat{c}$	dimensionless enrichment relative to the unweathered parent material of the immobile phase in the soil.
$\hat{c}_\eta$	dimensionless enrichment relative to the unweathered parent material of the immobile phase in the saprolite.
$\hat{c}_{\eta divide}$	dimensionless enrichment relative to the unweathered parent material of the immobile phase in the saprolite at the divide.
χ	increase in $\hat{c}$ as a function of position.
CDF	chemical depletion fraction (dimensionless).
δ_l	local error in the denudation ratio.
δ_I	integrated error in the denudation ratio.
d_ζ	deposition rate of sediment at soil surface ($L\ T^{-1}$).
D	sediment diffusivity ($L^2\ T^{-1}$).
η	elevation of soil-bedrock interface (L).
η_0	elevation of soil-bedrock interface at $x = 0$ (L).
η_{bl}	elevation of soil-bedrock interface relative to base level (L).
$\hat{\eta}$	dimensionless elevation of soil-bedrock interface relative to base level.
ϕ, $\hat{\phi}$	dimensional ($L^2\ T^{-1}$) and dimensionless sediment flux.
Φ_{dl}	local denudation ratio at the divide (dimensionless).

Φ_{sl} change in local denudation ratio over the hillslope (dimensionless).
γ soil production decay length scale (L).
h, $\hat{h}$ soil depth (L) and dimensionless soil depth, respectively.
I, $\hat{I}$ dimensional ($L\ T^{-1}$) and dimensionless incision rate, respectively $I = \partial\zeta_0/\partial t$.
K sediment dispersion coefficient ($M\ L^{-1}\ T^{-1}$).
λ length of the hillslope (half the distance between channels) (L).
m_i, m_{tot} mass of phase i and total mass of soil (M).
p_η Soil production rate ($L\ T^{-1}$).
$\overline{\rho}_s$ depth-averaged dry bulk density of hillslope soil ($M\ L^{-3}$).
ρ_η dry bulk density of parent material ($M\ L^{-3}$).
r_{ca}, r_c apparent and actual local rate of chemical denudation ($L\ T^{-1}$).
R_{ca}, R_c apparent and actual integrated rate of chemical denudation ($L\ T^{-1}$).
r_T local rate of total denudation ($L\ T^{-1}$).
R_T integrated rate of total denudation ($L\ T^{-1}$).
S_v chemical denudation and deposition rate per unit volume ($M\ L^{-3}\ T^{-1}$).
$\overline{S_v}$ depth-averaged chemical denudation rate per unit volume ($M\ L^{-3}\ T^{-1}$).
$\hat{S}$ dimensionless chemical denudation rate.
$\hat{S}_{divide}$ dimensionless chemical denudation rate at the divide.
σ change in $\hat{S}$ as a function of distance from the divide.
S_c critical slope (dimensionless).
θ_L length ratio (dimensionless).
θ_t time ratio (dimensionless).
Θ_{dl} local denudation ratio.
θ_d integrated denudation ratio.
θ_{da} apparent integrated denudation ratio.
τ_d density ratio (dimensionless).
T_p production timescale (T).
T_D diffusive (or relaxation) timescale (T).
T_R mean residence time of soil particles (T).
$\overline{v}_x$, $\overline{v}_y$ depth-averaged sediment velocity in the x and y direction ($L\ T^{-1}$).
W_0 nominal rate of soil production ($L\ T^{-1}$).
x, $\hat{x}$ dimensional (L) and dimensionless distance from the channel.
ζ elevation of soil surface (L).
ζ_0 elevation of soil surface at $x = 0$ (L).
ζ_{bl} elevation of soil surface relative to base level (L).
$\hat{\zeta}$ dimensionless elevation of soil surface relative to base level.

[43] **Acknowledgments.** This work was supported by the National Science Foundation (EAR-0125843). Kyungsoo Yoo's comments helped refine the direction of the manuscript. Discussions with Bill Dietrich about soil residence time helped inspire section 4.2. We thank Bob Anderson, Suzanne Anderson, and two anonymous referees for their careful and helpful reviews.

References

Ahnert, F. (1976), Brief description of a comprehensive three-dimensional process-response model of landform development, *Z. Geomorphol. Suppl.*, *25*, 29–49.

Amundson, R. (2004), Soil formation, in *Treatise on Geochemistry*, edited by H. D. Holland and K. K. Turekian, chap 5.01, pp. 1–35, Elsevier, New York.

Anderson, R. S. (2002), Modeling the tor-dotted crests, bedrock edges, and parabolic profiles of high alpine surfaces of the Wind River Range, Wyoming, *Geomorphology*, *46*(1–2), 35–58.

Anderson, S. P., W. E. Dietrich, and G. H. Brimhall (2002), Weathering profiles, mass-balance analysis, and rates of solute loss: Linkages between weathering and erosion in a small, steep catchment, *Geol. Soc. Am. Bull.*, *114*(9), 1143–1158.

Andrews, D. J., and R. C. Bucknam (1987), Fitting degradation of shoreline scarps by a nonlinear diffusion model, *J. Geophys. Res.*, *92*(B12), 12,857–12,867.

April, R., R. Newton, and L. T. Coles (1986), Chemical weathering in two Adirondack watersheds: Past and present-day rates, *Geol. Soc. Am. Bull.*, *97*(10), 1232–1238.

Armstrong, A. C. (1976), A three-dimensional simulation of slope forms, *Z. Geomorphol. Suppl.*, *25*, 20–28.

Berner, R. A., A. C. Lasaga, and R. M. Garrels (1983), The carbonate-silicate geochemical cycle and its effect on atmospheric carbon-dioxide over the past 100 million years, *Am. J. Sci.*, *283*(7), 641–683.

Birkeland, P. W. (1999), *Soils and Geomorphology*, 430 pp., Oxford Univ. Press, New York.

Brimhall, G. H., and W. E. Dietrich (1987), Constitutive mass balance relations between chemical-composition, volume, density, porosity, and strain in metasomatic hydrochemical systems: Results on weathering and pedogenesis, *Geochim. Cosmochim. Acta*, *51*(3), 567–587.

Brimhall, G. H., O. A. Chadwick, C. J. Lewis, W. Compston, I. S. Williams, K. J. Danti, W. E. Dietrich, M. E. Power, D. Hendricks, and J. Bratt (1992), Deformational mass-transport and invasive processes in soil evolution, *Science*, *255*(5045), 695–702.

Carson, M. A., and M. J. Kirkby (1972), *Hillslope Form and Process*, 475 pp., Cambridge Univ. Press, New York.

Chadwick, O. A., G. H. Brimhall, and D. M. Hendricks (1990), From a black box to a gray box: A mass balance interpretation of pedogenesis, *Geomorphology*, *3*, 369–390.

Culling, W. E. H. (1960), Analytical theory of erosion, *J. Geol.*, *68*(3), 336–344.

Culling, W. E. H. (1963), Soil creep and the development of hillside slopes, *J. Geol.*, *71*(2), 127–161.

Fernandes, N. F., and W. E. Dietrich (1997), Hillslope evolution by diffusive processes: The timescale for equilibrium adjustments, *Water Resour. Res.*, *33*(6), 1307–1318.

Furbish, D. J., and S. Fagherazzi (2001), Stability of creeping soil and implications for hillslope evolution, *Water Resour. Res.*, *37*(10), 2607–2618.

Gabet, E. J. (2000), Gopher bioturbation: Field evidence for non-linear hillslope diffusion, *Earth Surf. Processes Landforms*, *25*(13), 1419–1428.

Gabet, E. J., O. J. Reichman, and E. W. Seabloom (2003), The effects of bioturbation on soil processes and sediment transport, *Annu. Rev. Earth Planet. Sci.*, *31*, 249–273.

Gilbert, G. K. (1877), *Report on the Geology of the Henry Mountains: U.S. Geographical and Geological Survey of the Rocky Mountain Interior Region*, 160 pp., U.S. Gov. Print. Off., Washington, D. C.

Gilbert, G. K. (1909), The convexity of hilltops, *J. Geol.*, *17*, 344–350.

Green, E. G., W. E. Dietrich, and J. F. Banfield (2005), Quantification of chemical weathering rates across an actively eroding hillslope, *Earth Planet. Sci. Lett.*, *242*, 155–169, doi:10.1016/j.epsl.2005.11.039.

Heimsath, A. M., W. E. Dietrich, K. Nishiizumi, and R. C. Finkel (1997), The soil production function and landscape equilibrium, *Nature*, *388*(6640), 358–361.

Heimsath, A. M., W. E. Dietrich, K. Nishiizumi, and R. C. Finkel (1999), Cosmogenic nuclides, topography, and the spatial variation of soil depth, *Geomorphology*, *27*(1–2), 151–172.

Heimsath, A. M., J. Chappell, W. E. Dietrich, K. Nishiizumi, and R. C. Finkel (2000), Soil production on a retreating escarpment in southeastern Australia, *Geology*, *28*(9), 787–790.

Heimsath, A. M., W. E. Dietrich, K. Nishiizumi, and R. C. Finkel (2001), Stochastic processes of soil production and transport: Erosion rates, topographic variation and cosmogenic nuclides in the Oregon Coast Range, *Earth Surf. Processes Landforms*, *26*(5), 531–552.

Jyotsna, R., and P. K. Haff (1997), Microtopography as an indicator of modern hillslope diffusivity in arid terrain, *Geology*, *25*(8), 695–698.

Kirchner, J. W., R. C. Finkel, C. S. Riebe, D. E. Granger, J. L. Clayton, J. G. King, and W. F. Megahan (2001), Mountain erosion over 10 yr, 10 k.y., and 10 m.y. time scales, *Geology*, *29*(7), 591–594.

Kirkby, M. J. (1967), Measurement and theory of soil creep, *J. Geol.*, *75*(4), 359–378.

Kirkby, M. J. (1971), Hillslope process-response models based on the continuity equation, *Inst. Br. Geogr. Spec. Publ.*, *3*, 15–30.

Kirkby, M. J. (1977), Soil development models as a component of slope models, *Earth Surf. Processes Landforms*, *2*(2–3), 203–230.

Kirkby, M. J. (1985a), A basis for soil-profile modeling in a geomorphic context, *J. Soil Sci.*, *36*(1), 97–121.

Kirkby, M. J. (1985b), A model for the evolution of regolith-mantled slopes, in *Models in Geomorphology*, edited by M. J. Woldenberg, pp. 213–237, Allen and Unwin, St. Leonards, N.S.W., Australia.

Merritts, D. J., O. A. Chadwick, D. M. Hendricks, G. H. Brimhall, and C. J. Lewis (1992), The mass balance of soil evolution on late Quaternary marine terraces, northern California, *Geol. Soc. Am. Bull.*, *104*(11), 1456–1470.

Mudd, S. M., and D. J. Furbish (2004), The influence of chemical denudation on hillslope morphology, *J. Geophys. Res.*, *109*, F02001, doi:10.1029/2003JF000087.

Mudd, S. M., and D. J. Furbish (2005), Lateral migration of hillcrests in response to channel incision in soil-mantled landscapes, *J. Geophys. Res.*, *110*, F04026, doi:10.1029/2005JF000313.

Nezat, C. A., J. D. Blum, A. Klaue, C. E. Johnson, and T. G. Siccama (2004), Influence of landscape position and vegetation on long-term weathering rates at the Hubbard Brook Experimental Forest, New Hampshire, USA, *Geochim. Cosmochim. Acta*, *68*(14), 3065–3078.

Paola, C., and V. R. Voller (2005), A generalized Exner equation for sediment mass balance, *J. Geophys. Res.*, *110*, F04014, doi:10.1029/2004JF000274.

Raymo, M. E., and W. F. Ruddiman (1992), Tectonic forcing of late Cenozoic climate, *Nature*, *359*(6391), 117–122.

Riebe, C. S., J. W. Kirchner, D. E. Granger, and R. C. Finkel (2001), Strong tectonic and weak climatic control of long-term chemical weathering rates, *Geology*, *29*(6), 511–514.

Riebe, C. S., J. W. Kirchner, and R. C. Finkel (2003), Long-term rates of chemical weathering and physical erosion from cosmogenic nuclides and geochemical mass balance, *Geochim. Cosmochim. Acta*, *67*(22), 4411–4427.

Riebe, C. S., J. W. Kirchner, and R. C. Finkel (2004a), Erosional and climatic effects on long-term chemical weathering rates in granitic landscapes spanning diverse climate regimes, *Earth Planet. Sci. Lett.*, *224*(3–4), 547–562.

Riebe, C. S., J. W. Kirchner, and R. C. Finkel (2004b), Sharp decrease in long-term chemical weathering rates along an altitudinal transect, *Earth Planet. Sci. Lett.*, *218*(3–4), 421–434.

Roering, J. J. (2004), Soil creep and convex-upward velocity profiles: Theoretical and experimental investigation of disturbance-driven sediment transport on hillslopes, *Earth Surf. Processes Landforms*, *29*(13), 1597–1612.

Roering, J. J., J. W. Kirchner, and W. E. Dietrich (1999), Evidence for nonlinear, diffusive sediment transport on hillslopes and implications for landscape morphology, *Water Resour. Res.*, *35*(3), 853–870.

Roering, J. J., J. W. Kirchner, and W. E. Dietrich (2001), Hillslope evolution by nonlinear, slope-dependent transport: Steady state morphology and equilibrium adjustment timescales, *J. Geophys. Res.*, *106*(B8), 16,499–16,513.

Small, E. E., R. S. Anderson, J. L. Repka, and R. Finkel (1997), Erosion rates of alpine bedrock summit surfaces deduced from in situ ^{10}Be and ^{26}Al, *Earth Planet. Sci. Lett.*, *150*, 413–425.

Small, E. E., R. S. Anderson, and G. S. Hancock (1999), Estimates of the rate of regolith production using Be-10 and Al-26 from an alpine hillslope, *Geomorphology*, *27*(1–2), 131–150.

Stallard, R. F. (1995), Tectonic, environmental, and human aspects of weathering and erosion: A global review using a steady-state perspective, *Annu. Rev. Earth Planet. Sci.*, *23*, 11–39.

Taylor, A., and J. D. Blum (1995), Relation between soil age and silicate weathering rates determined from the chemical evolution of a glacial chronosequence, *Geology*, *23*(11), 979–982.

West, A. J., A. Galy, and M. Bickle (2005), Tectonic and climatic controls on silicate weathering, *Earth Planet. Sci. Lett.*, *235*(1–2), 211–228.

White, A. F., and S. L. Brantley (1995), Chemical weathering rates of silicate minerals: An overview, in *Chemical Weathering Rates of Silicate Minerals*, vol. 31, edited by A. F. White and S. L. Brantley, pp. 1–22, Mineral. Soc. of Am., Washington, D. C.

White, A., and S. L. Brantley (2003), The effect of time on the weathering of silicate minerals: Why do weathering rates differ in the laboratory and field?, *Chem. Geol.*, *202*, 479–506.

White, A. F., A. E. Blum, M. S. Schulz, D. V. Vivit, D. A. Stonestrom, M. Larsen, S. F. Murphy, and D. Eberl (1998), Chemical weathering in a tropical watershed, Luquillo Mountains, Puerto Rico: I. Long-term versus short-term weathering fluxes, *Geochim. Cosmochim. Acta*, *62*(2), 209–226.

Wilkinson, M. T., J. Chappell, G. S. Humphreys, K. Fifield, B. Smith, and P. Hesse (2005), Soil production in heath and forest, Blue Mountains, Australia: Influence of lithology and palaeoclimate, *Earth Surf. Processes Landforms*, *30*(8), 923–934.

Yoo, K., R. Amundson, A. M. Heimsath, W. E. Dietrich, and G. H. Brimhall (2004), The topographic control of chemical weathering in hillslope soils, *Eos Trans. AGU*, *85*(47), Fall Meet. Suppl., Abstract H41H-05.

D. J. Furbish, Department of Earth and Environmental Sciences, Vanderbilt University, Nashville, TN 37235, USA.

S. M. Mudd, Department of Civil and Environmental Engineering, Vanderbilt University, Nashville, TN 37235, USA. (simon.m.mudd@vanderbilt.edu)